Supplementary Information

Molecular Insights into How the Motions of the β-Barrel and POTRA Domains of BamA Are Coupled for Efficient Function

Naemi Csoma[1,2,$], Jonathan M. Machin[3,$], James M. Whitehouse[3,$], Raquel Rodrìguez-Alonso[1,2], Monika Olejnik[3], Adam K. Cahill[3], Seung-Hyun Cho[1,2], Till F. Schäberle[4,5,6], Bogdan I. Iorga[2,7], Neil A. Ranson[3], Sheena E. Radford[3]*, Antonio N. Calabrese[3]*, Jean-François Collet[1,2]*

[1]WELBIO department, WEL Research Institute, avenue Pasteur, 6, 1300 Wavre, Belgium

[2]de Duve Institute, Université catholique de Louvain (UCLouvain), Avenue Hippocrate 75, 1200 Brussels, Belgium

[3]Astbury Centre for Structural Molecular Biology, School of Molecular and Cellular Biology, Faculty of Biological Sciences, University of Leeds, Leeds, UK

[4]Institute for Insect Biotechnology, Justus-Liebig-University Giessen, 35392 Giessen, Germany

[5]German Center for Infection Research (DZIF), Partner Site Giessen-Marburg-Langen, 35392 Giessen, Germany

[6]Branch for Bioresources, Fraunhofer Institute for Molecular Biology and Applied Ecology (IME), 35392 Giessen, Germany

[7]Université Paris-Saclay, Institut de Chimie des Substances Naturelles, Gif-sur-Yvette, France

$ These authors contributed equally

*Correspondence: s.e.radford@leeds.ac.uk (S.E.R), a.calabrese@leeds.ac.uk (A.N.C), jfcollet@uclouvain.be (J.-F.C.)

Supplementary Table 1 | Folding yields for tOmpA and OmpX after 3 hours or 24 hours for different BAM variants

Folding yield data are reported as the mean of two biological replicates. The range of values covered by the replicates is also reported.

Variant	Time (hours)	**tOmpA**		**OmpX**	
		Folding yield after 3 or 24 hours (%)	Range (%)	Folding yield after 3 or 24 hours (%)	Range (%)
BAM_{WT}	3	96%	1%	84%	18%
BAM_{LVPR}	3	54%	0%	30%	7%
BAM_{GSGS}	3	75%	1%	28%	0%
BAM_{WT}	24	100%	0%	93%	3%
BAM_{LVPR}	24	70%	21%	74%	14%
BAM_{GSGS}	24	90%	7%	79%	1%

Supplementary Table 2 | Initial folding rates for tOmpA and OmpX at 25 °C for each BAM variant

OMP substrates were folded into *E. coli* polar lipid proteoliposomes in TBS pH 8.0 at 25 °C in the presence of the various BAM variants. Each experiment was repeated at least once, as stated to confirm reproducibility (note that more replicates were included for WT BAM as this construct was included as a control when each variant was assayed.) Initial rates were calculated independently for each replicate with the range of values (maximum – minimum) shown to highlight reproducibility. The initial rates presented show the average of (n) repeat experiments. Initial rates as a percentage of the WT BAM initial rate are also shown for each variant.

Variant	tOmpA				OmpX			
	Initial rate (s^{-1})	Range (s^{-1})	Number of replicates (n)	Rel. to WT BAM (%)	Initial rate (s^{-1})	Range (s^{-1})	Number of replicates (n)	Rel. to WT BAM (%)
WT BAM	7.12×10^{-4}	5.81×10^{-5}	4	100	2.20×10^{-4}	1.24×10^{-4}	7	100
BAM_{LVPR}	9.79×10^{-5}	2.28×10^{-5}	2	14	4.15×10^{-5}	3.31×10^{-6}	2	19
BAM_{GSGS}	1.85×10^{-4}	3.26×10^{-5}	2	26	4.02×10^{-5}	4.94×10^{-6}	2	18

Supplementary Table 3 | Folding yields for tOmpA and OmpX 24 hours in presence of darobactin

Folding yield data are reported as the mean of two biological replicates. The range of values covered by the replicates is also reported.

Variant	**tOmpA**		**OmpX**	
	Folding yield after 24 hours (%)	Range (%)	Folding yield after 24 hours (%)	Range (%)
BAM + DMSO	99%	1%	-	-
BAM	100%	0%	100%	0%
BAM + DarB	63%	1%	5%	7%
BAM_{T434A}	100%	0%	100%	0%
BAM_{T434A} + DarB	80%	0%	37%	1%

Supplementary Table 4 | Strains used in this study

Strains	Genotype and description	Source
BL21 (DE3)	F- *ompT hsdSB* (rB- mB-) *gal dcm* (DE3)	Novagen
DH300	*rprA-lacZ* MG1655 *(argF-lac) U169*	[1]
CAG45114	MG1655 ΔlacX74 Fl(rpoHP3-LacZ)	[2]
SEN1603	DH300 *bamA::kan* with pBamA	[3]
SEN1722	DH300 *bamA::kan* with $pBamA_{LVPR}$	[3]
NCAs580	CAG45114 *bamA::kan* with pBamA	This study
NCAs584	CAG45114 *bamA::kan* with $pBamA_{T434A}$	This study
NCAs595	CAG45114 *bamA::kan* with $pBamA_{GSGS}$	This study
NCAs596	CAG45114 *bamA::kan* with $pBamA_{LVPR*}$	This study
NCAs597	CAG45114 *bamA::kan* with $pBamA_{LVPR}$	This study
JMW01	BL21 with pJH114	This study
JMW02	BL21 with pNCA161	This study
JMW03	BL21 with pNCA162	This study
JMW04	BL21 with pRRA3	This study

Supplementary Table 5 | Plasmids used in this study

Plasmids	Features	Source
pBamA	pET23a with BamAss-6xHis-2xAla-$BamA_{(E22\text{-}W810)}$, Ampicillin	[4]
$pBamA_{LVPR}$	pBamA (BamA with the insertion of a LVPR sequence at position 424)	[3]
$pBamA_{GSGS}$	pBamA (BamA with the insertion of a GSGS sequence at position 424)	This study
$pBamA_{LVPR*}$	pBamA (BamA with the insertion of an LVPR sequence at position 424 and the substitution of threonine with alanine at position 434)	This study
$pBamA_{T434A}$	pBamA (BamA with the substitution of threonine with alanine at position 434)	This study
pJH114	pTrc99 (BamA-BamB-BamC-BamD-BamE- 8×His)	[5]
pNCA161	pJH114 but with modifications: T434A point mutation	This study
pNCA162	pJH114 but with modifications: BamA with the insertion of LVPR sequence at position 424	This study
pRRA3	pJH114 but with modifications: BamA with the insertion of GSGS sequence at position 424	This study

Supplementary Table 6 | Primers used in this study

Name	Sequence (5’ to 3’)
BamA hinge F	GTAAAAGAGCGCAACACCCTGGTGCCGCGCGGTAGC TTCAACTTTGGT
BamA hinge R	ACCAAAGTTGAAGCTACCGCGCGGCACCAGGGTGTT GCGCTCTTTTAC
RRA93-bamA GSGS-F	CACCGGGTCTGGGTCTGGTAGCTTCAAC
RRA94-bamA GSGS-R	ACCAGACCCAGACCCGGTGTTGCGCTC
RRA97-BamAT434A-F	ACGTAATTTAACGGCTTTGTCGGCATCGTTAATTTCGGG
RRA98-BamAT434A-R	CCCGAAATTAACGATGCCGACAAAGCCGTTAAATTACGT

Supplementary Data 1 | Diverse dataset of 3992 complete RefSeq bacterial genomes with phylogenetic details

Attached Excel Sheet

Supplementary Data 2 | Correspondence between RefSeq and UniProt accessions for BamA from different species, with the list of corresponding AlphaFold2 predicted structures

Attached Excel Sheet

Supplementary Table 7| Molecular Dynamics Checklist

Reliability and reproducibility checklist for molecular dynamics simulations ***All boxes must be marked YES by acceptance unless "Response not needed if No".**	**Yes**	**No**	**Response**
1. Convergence of simulations and analysis			
1a. Is an evaluation presented in the text to show that the property being measured has equilibrated in the simulations (*e.g.* time-course analysis)?	☒	☐	The distribution is the same in the three replica simulations, as shown in Figure 1g.
1b. Then, is it described in the text how simulations are split into equilibration and production runs and how much data were analyzed from production runs?	☒	☐	Section "Methods"/"Molecular dynamics simulations"
1c. Are there at least 3 simulations per simulation condition with statistical analysis?	☒	☐	Section "Methods"/"Molecular dynamics simulations" and Figure 1g.
1d. Is evidence provided in the text that the simulation results presented are independent of initial configuration?	☒	☐	Different seed values were used during the preparation of the simulations, so they are independent.
2. Connection to experiments			
2a. Are calculations provided that can connect to experiments (*e.g.* loss or gain in function from mutagenesis, binding assays, NMR chemical shifts, J-couplings, SAXS curves, interaction distances or FRET distances, structure factors, diffusion coefficients, bulk modulus and other mechanical properties, *etc*.)?	☒	☐	The distribution of dihedral angles values obtained from the simulations are coherent with those expected for polypeptide systems.
3. Method choice			
3a. Do simulations contain membranes, membrane proteins, intrinsically disordered proteins, glycans, nucleic acids, polymers, or cryptic ligand binding?	☐	☒	
3b. Is it described in the text whether the accuracy of the chosen model(s) is sufficient to address the question(s) under investigation (e.g. all-atom vs. coarse-grained models, fixed charge vs. polarizable force fields, implicit vs. explicit solvent or membrane, force field and water model, etc.)?	☒	☐	The simulations are performed using state-of-the-art software, models and parameters.
3c. Is the timescale of the event(s) under investigation beyond the brute-force MD simulation timescale in this study that enhanced sampling methods are needed?	☐	☒	

	If **YES**, are the parameters and convergence criteria for the enhanced sampling method clearly stated?	☐	☐	
	If **NO,** is the evidence provided in the text?	☒	☐	The distribution is the same in the three replica simulations, as shown in Figure 1g.
4. Code and reproducibility				
4a. Is a table provided describing the system setup that includes simulation box dimensions, total number of atoms, total number of water molecules, salt concentration, lipid composition (number of molecules and type)?		☒	☐	This information is not provided as a table but the simulations files were deposited in a public repository [https://github.com/IorgaLab/BamAset , https://doi.org/10.5281/zenodo.13986908] [6].
4b. Is it described in the text what simulation and analysis software and which versions are used?		☒	☐	Section "Methods"/"Molecular dynamics simulations"
4c. Are other parameters for the system setup described in the text, such as protonation state, type of structural restraints if applied, nonbonded cutoff, thermostat and barostat, etc.?		☒	☐	Section "Methods"/"Molecular dynamics simulations"
4d. Are initial coordinate and simulation input files and a coordinate file of the final output provided as supplementary files or in a public repository?		☒	☐	The simulations files were deposited in a public repository [https://github.com/IorgaLab/BamAset , , https://doi.org/10.5281/zenodo.13986908] [6].
4e. Is there custom code or custom force field parameters?		☐	☒	
	If **YES**, are they provided as supplementary files or in a public repository?	☐	☐	

Supplementary Table 8 | CryoEM data collection, refinement, validation and model building statistics.

	BAM_{LVPR} (EMD-51930) (PDB ID 9H84)	BAM_{GSGS} (EMD-51931) (PDB ID 9H85)	BAM_{LVPR}-T434A (EMD-51933) (PDB ID 9H89)
Data collection and processing			
Magnification	96k	130k	130k
Voltage (kV)	300	300	300
Electron exposure (e–/Å^2)	35.7	40.0	39.8
Defocus range (μm)	-0.9 to -3.0	-0.9 to -3.0	-0.9 to -3.0
Pixel size (Å)	0.83	0.87	0.91
Micrograph number	1850	7813	1504
Symmetry imposed	C1	C1	C1
Initial particle images (no.)	421, 707	975, 473	164, 998
Final particle images (no.)	127, 056	75, 557	62, 266
Map resolution (Å)	4.3	4.2	4.0
0.143 FSC threshold			
Map resolution range (Å)	3.9-11.5	4.0-7.5	3.7-10.6
Refinement			
Initial model used (PDB code)	8BWC/5D0O	BAM_{LVPR}	BAM_{LVPR}
Map sharpening *B* factor (Å^2)	-147	-60	-10
Model composition			
Non-hydrogen atoms	11496	11501	11494
Protein residues	1472	1474	1472
R.M.S. deviations			
Bond lengths (Å)	0.004	0.006	0.002
Bond angles (°)	0.985	1.068	0.603
Validation			
MolProbity score	1.91	1.42	1.76
Clashscore	11.97	2.79	10.02
Poor rotamers (%)	0.16	0	0.16
Ramachandran plot			
Favored (%)	95.42	94.95	96.37
Allowed (%)	4.44	4.98	3.63
Outliers (%)	0.14	0.07	0

Supplementary Table 9| HDX Data Summary TableS

D = standard deviation, CI = confidence interval.

Data Set	BAM	BAM_{LVPR}	BAM_{T434A}
HDX reaction details	10 mM potassium phosphate, pH 8.0, 0.02% n-dodecyl-β-d-Maltoside (DDM)		
HDX time course (min)	0.5, 2, 30 min		
HDX control samples	Maximally-labelled controls were not performed.		
Back-exchange	~ 40 %		
# of Peptides	BamA: 170 BamB: 55 BamC: 51 BamD: 31 BamE:4	BamA: 170 BamB: 55 BamC: 51 BamD: 31 BamE:4	BamA: 170 BamB: 55 BamC: 51 BamD: 31 BamE:4
Sequence coverage	BamA: 80.0 % BamB: 75.3 % BamC 87.5 % BamD: 71.2 % BamE: 54.2 %	BamA: 80.0 % BamB: 75.3 % BamC 87.5 % BamD: 71.2 % BamE: 54.2 %	BamA: 80.0 % BamB: 75.3 % BamC 87.5 % BamD: 71.2 % BamE: 54.2 %
Average peptide length / Redundancy	BamA: 10.66 / 2.87 BamB: 11.16 / 2.19 BamC: 12.04 / 2.19 BamD: 9.39 / 1.81 BamE: 14.50 / 1.12	BamA: 10.66 / 2.87 BamB: 11.16 / 2.19 BamC: 12.04 / 2.19 BamD: 9.39 / 1.81 BamE: 14.50 / 1.12	BamA: 10.66 / 2.87 BamB: 11.16 / 2.19 BamC: 12.04 / 2.19 BamD: 9.39 / 1.81 BamE: 14.50 / 1.12
Replicates	3 (technical)	3 (technical)	3 (technical)
Repeatability (average SD)	BamA: 0.0752 BamB: 0.0705 BamC: 0.0809 BamD: 0.0714 BamE: 0.1016	BamA: 0.0643 BamB: 0.0480 BamC: 0.0756 BamD: 0.0594 BamE: 0.0742	BamA: 0.0734 BamB: 0.0610 BamC: 0.0810 BamD: 0.0790 BamE: 0.0886
Significant differences in HDX (delta HDX > X D)	Hybrid significance test: 95 % CI, $p < 0.05$ See Supplementary Figures 10-14 for delta HDX values for each comparison.		

Supplementary Figures

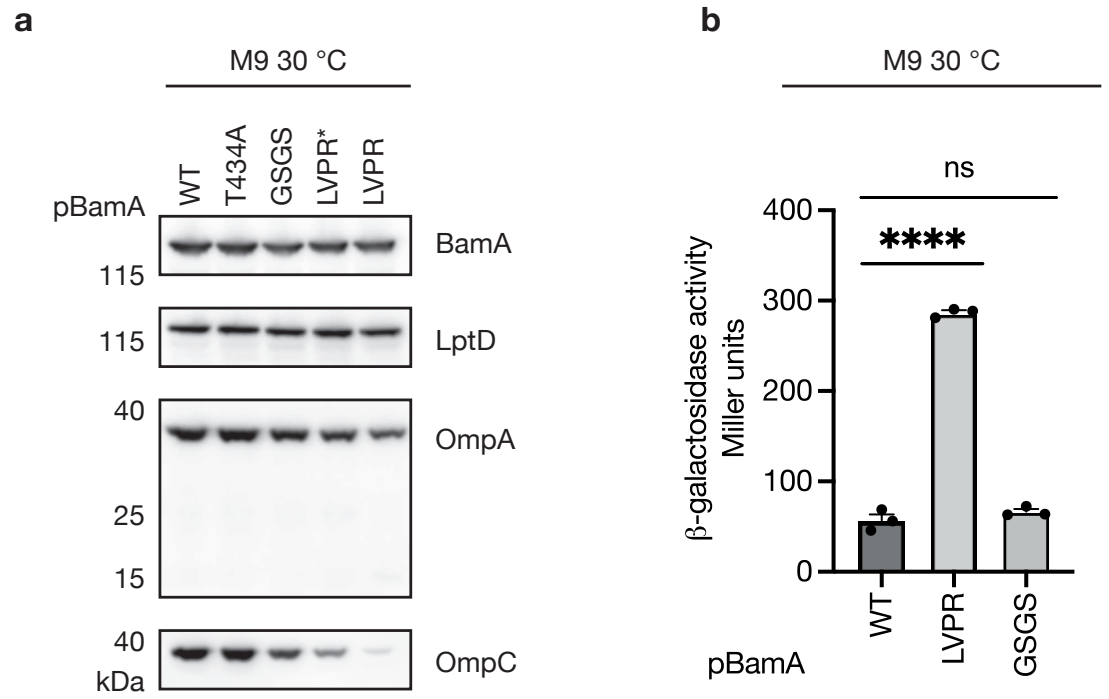

Supplementary Figure 1
Rigidifying the hinge region of BamA is deleterious to BAM function
a and **b** $BamA_{LVPR}$ impairs OMP folding leading to activation of the SigmaE response, while $BamA_{GSGS}$ has no effect on BAM function at 30 °C in minimal medium suggesting that the rigidity of the LVPR insertion causes the defects observed. Cells were grown in M9 minimal medium at 30 °C until mid-log phase. **a** Western blot analysis of trichloroacetic acid (TCA) precipitates of annotated cells. Nitrocellulose membranes were probed with primary antibody targeted against proteins mentioned on the right. Samples were normalized by the OD_{600} of their cultures. Representative data of three biological replicates. **b** SigmaE activity measured by β-galactosidase assay was reported using the transcriptional rpoHP3'-lacZ fusion on the chromosome. Error bars represent standard error of the mean (n=3 biological replicates). P-values were evaluated by a mixed model, with random plate effect, and multiple comparisons with adjustment by the Dunnet method (****p<0.0001, ns: non-significant).

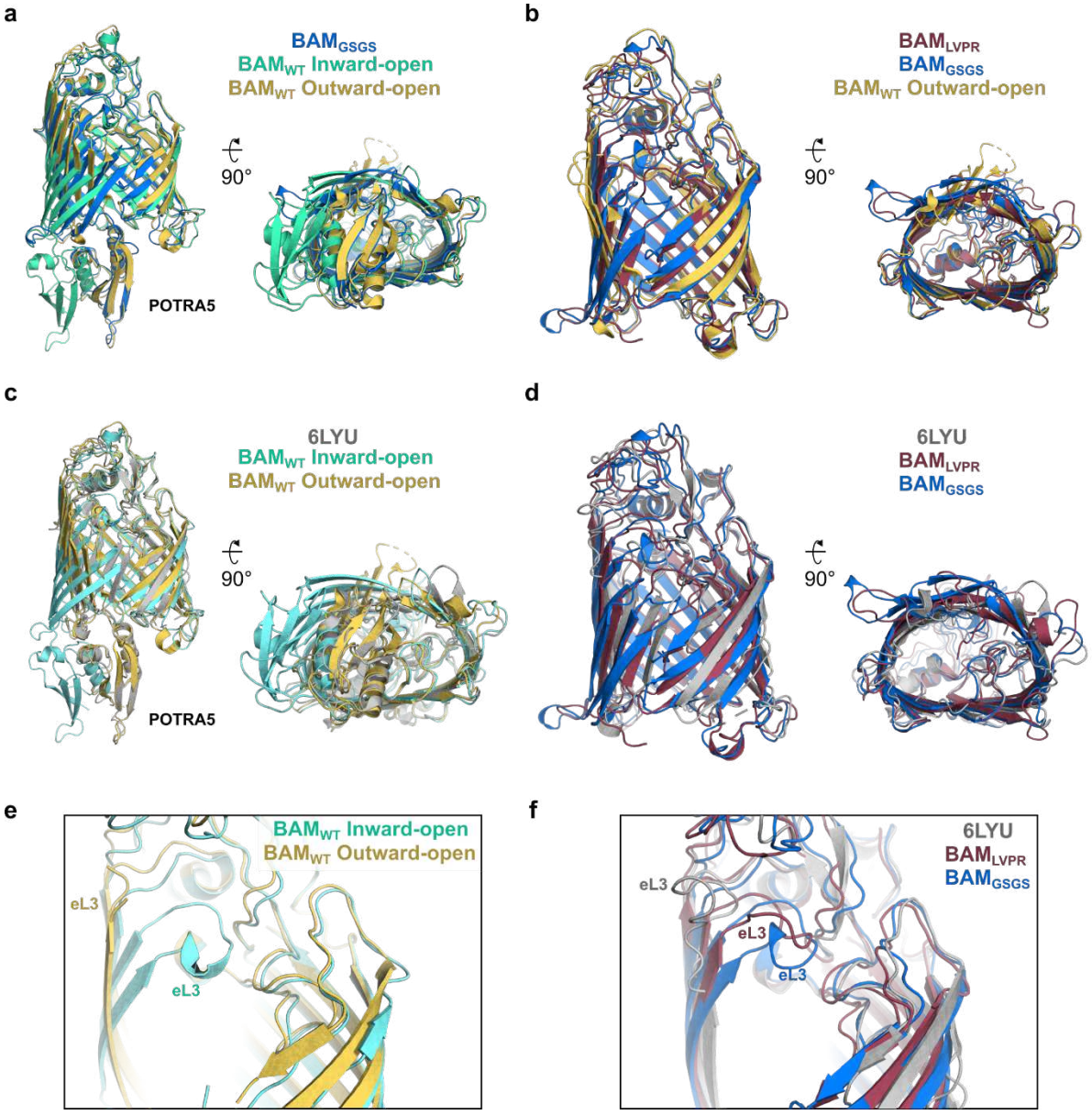

Supplementary Figure 2

Additional structural comparisons of BAM_{LVPR}/BAM_{GSGS} to published BAM structures

a Comparison between BamA of canonical inward-open and outward-open and BAM_{GSGS}, only the transmembrane domain and POTRA5 are shown for clarity. **b** Comparison between the transmembrane domains of BAM_{LVPR}, BAM_{GSGS} and BAM-WT outward-open, showing lateral-gate closure. **c** Comparison between a nanodisc BAM-WT structure, which also shows lateral-gate closure and periplasmic domains in the inward-open conformation (6LYU), and canonical inward-open and outward-open structures. Only the transmembrane domain and POTRA5 are shown for clarity. **d** Comparison between BAM_{LVPR}, BAM_{GSGS} and 6LYU transmembrane barrel domains. **e** Comparison of extracellular loop 3 (eL3) in inward-open and outward-open conformations, demonstrating the ordering and folding inwards of the loop as the barrel closes in the inward-open conformation (β1-4 and eL1-2 not shown for clarity). **f** Comparison of BAM_{LVPR} and BAM_{GSGS} with 6LYU, demonstrating the inward-open like conformation of eL3 in $BAM_{LVPR/GSGS}$ but not in 6LYU. PDBs: 8BWC[7] (outward-open), 5D0O[8] (inward-open), 6LYU[9].

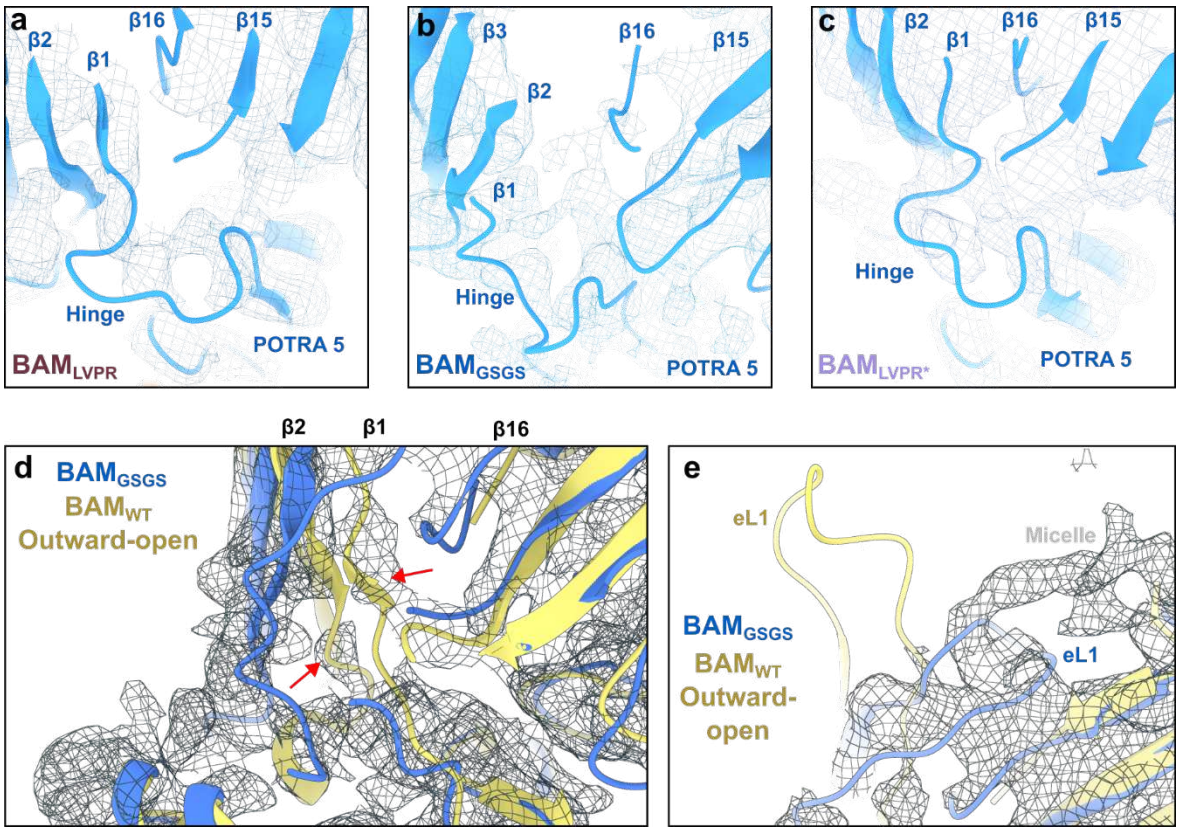

Supplementary Figure 3

The hinge region is poorly resolved in all cryoEM models

Density for the hinge region showing its poorly resolved nature for **a** BAM_{LVPR}, **b** BAM_{GSGS} and **c** BAM_{LVPR}*. Only BamA shown for clarity. Even at low contour, there is minimal density for the hinge region, indicating high levels of disorder in this region. Linker regions were flexibly fitted into the available density and energy minimized, but do not show a definitive path. **d** Base and **e** top of the barrel at the β-seam region comparing the density for the BAM_{GSGS} map to the fitted model and the outward-open structure. At low map contour, red arrows in **d** indicate evidence of a more outward-open like conformation at the base of the barrel, but not at the top of the barrel **e**.

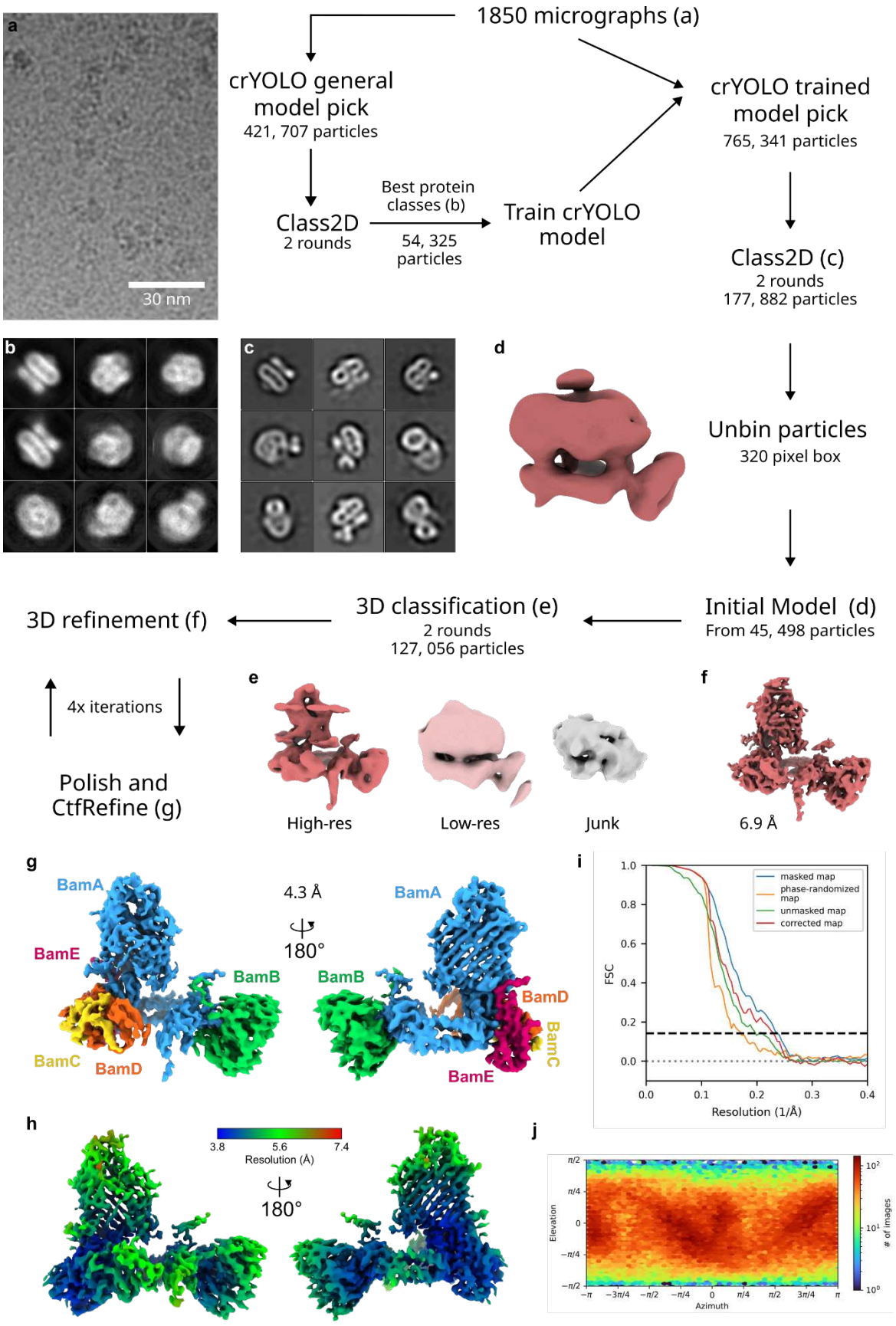
a
30 nm
1850 micrographs (a)
crYOLO general model pick
421, 707 particles
Class2D
2 rounds
Best protein classes (b)
54, 325 particles
Train crYOLO model
crYOLO trained model pick
765, 341 particles
Class2D (c)
2 rounds
177, 882 particles
b
c
d
Unbin particles
320 pixel box
Initial Model (d)
From 45, 498 particles
3D classification (e)
2 rounds
127, 056 particles
3D refinement (f)
4x iterations
Polish and CtfRefine (g)
e
High-res
Low-res
Junk
f
6.9 Å
g
BamA
BamE
BamB
BamC
BamD
4.3 Å
180°
i
masked map
phase-randomized map
unmasked map
corrected map
FSC
Resolution (1/Å)
h
3.8
5.6
7.4
Resolution (Å)
180°
j
Elevation
Azimuth
# of images

Supplementary Figure 4

CryoEM processing workflow for BAM_{LVPR}

a Micrographs were picked using crYOLO's general model, and the resulting protein-like 2D classes **b** were used to train a crYOLO model, yielding a higher and cleaner particle count **c**. Initial model generation **d** and 3D classifications **e** yielded as expected lower resolution models. 3D refinement followed by 4x rounds of polishing improved the final model to a global resolution of 4.3 Å **f**-**g**, and local resolution estimates shown in **h**. **I** The FSC curves of the model and **j** the particle orientation distribution (generated in cryoSPARC).

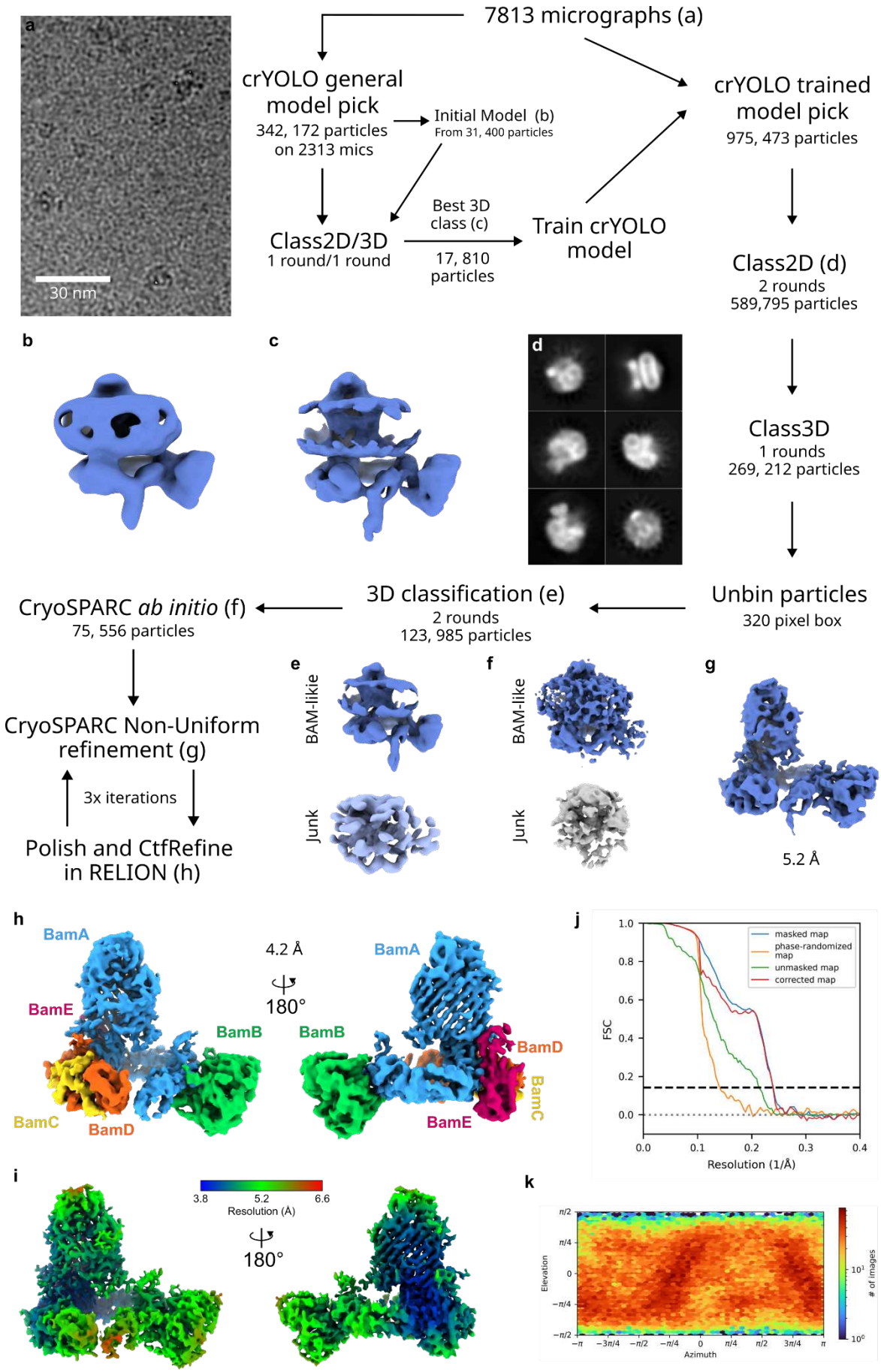
a
30 nm
7813 micrographs (a)
crYOLO general model pick
342, 172 particles on 2313 mics
Initial Model (b)
From 31, 400 particles
crYOLO trained model pick
975, 473 particles
Class2D/3D
1 round/1 round
Best 3D class (c)
17, 810 particles
Train crYOLO model
Class2D (d)
2 rounds
589,795 particles
b
c
d
Class3D
1 rounds
269, 212 particles
Unbin particles
320 pixel box
3D classification (e)
2 rounds
123, 985 particles
CryoSPARC ab initio (f)
75, 556 particles
CryoSPARC Non-Uniform refinement (g)
3x iterations
Polish and CtfRefine in RELION (h)
e
BAM-likie
Junk
f
BAM-like
Junk
g
5.2 Å
h
BamA
BamE
BamB
BamC
BamD
4.2 Å
180°
BamA
BamB
BamD
BamC
BamE
j
masked map
phase-randomized map
unmasked map
corrected map
FSC
Resolution (1/Å)
i
3.8
5.2
6.6
Resolution (Å)
180°
k
Elevation
Azimuth
# of images

Supplementary Figure 5

CryoEM processing workflow for BAM_{GSGS}

a Micrographs were picked using crYOLO's general model, and particles contributing to the resulting BAM-like first-pass 3D class **c**-**b** were used to train a crYOLO model, yielding a higher and cleaner particle count **d**. 3D classifications **e** and cryoSPARC *ab initio* model generation **f** further cleaned up the particle stack. Three iterations of Non-Uniform refinements and particle polishing improved the final model to a global resolution of 4.2 Å **g**-**h**, and local resolution estimates shown in **i**. **j** The FSC curves of the model and **k** the particle orientation distribution (generated in cryoSPARC).

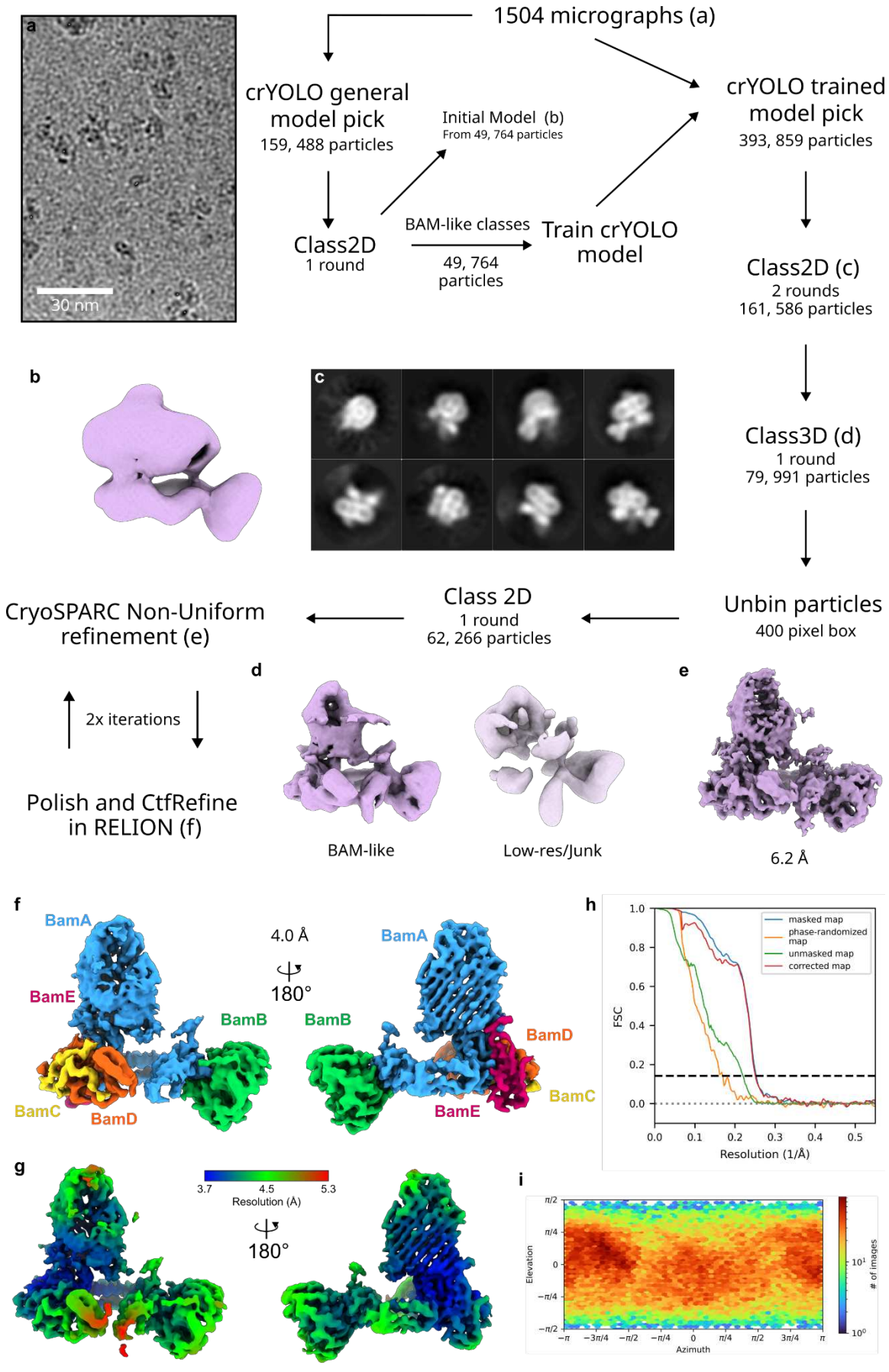
a
30 nm
1504 micrographs (a)
crYOLO general model pick
159, 488 particles
Initial Model (b)
From 49, 764 particles
crYOLO trained model pick
393, 859 particles
Class2D
1 round
BAM-like classes
49, 764 particles
Train crYOLO model
Class2D (c)
2 rounds
161, 586 particles
b
c
Class3D (d)
1 round
79, 991 particles
Unbin particles
400 pixel box
Class 2D
1 round
62, 266 particles
CryoSPARC Non-Uniform refinement (e)
2x iterations
Polish and CtfRefine in RELION (f)
d
BAM-like
Low-res/Junk
e
6.2 Å
f
BamA
BamE
BamB
BamC
BamD
4.0 Å
180°
g
3.7
4.5
5.3
Resolution (Å)
180°
h
masked map
phase-randomized map
unmasked map
corrected map
FSC
Resolution (1/Å)
i
Elevation
Azimuth
# of images

Supplementary Figure 6

CryoEM processing workflow for BAM_{LVPR}*

a Micrographs were picked using crYOLO's general model, and particles contributing to a BAM-like initial model **b** were used to train a crYOLO model, yielding a higher and cleaner particle count **c**. 3D classifications **d** further cleaned up the particle stack. Two iterations of Non-Uniform refinements and particle polishing improved the final model to a global resolution of 4.0 Å **e-f**, and local resolution estimates shown in **g**. **h** The FSC curves of the model and **i** the particle orientation distribution (generated in cryoSPARC).

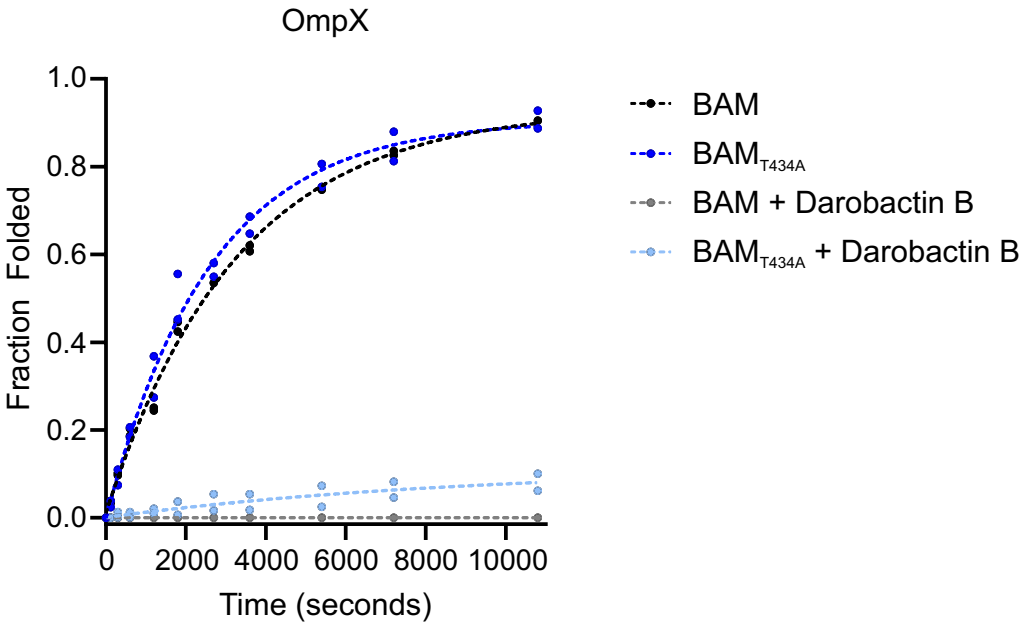

Supplementary Figure 7

The BamA T434A mutation decreases the effect of darobactin B on the folding activity of BAM in an *in vitro* folding assay

Quantification of the folded fraction of OmpX against time, from the SDS-PAGE band-shift assay. Data markers represent the folded fraction values calculated from two repeat measurements and dashed lines represent the single exponential fit to the data.

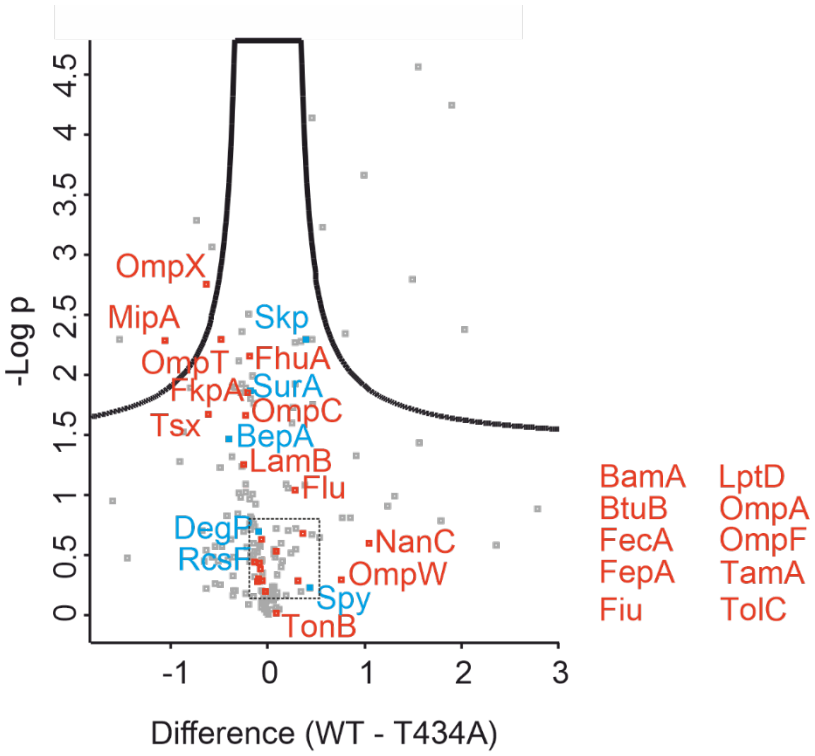

Supplementary Figure 8

Cells expressing BamA$_{T434A}$ have minimal outer membrane defects

Volcano plot showing the difference in protein expression levels between cells expressing WT BamA or BamA$_{T434A}$. Volcano plot shows data for detected proteins with GO terms associated with the periplasm, outer membrane or peptidoglycan layer. OMPs are labelled in red and periplasmic chaperones and stress-related proteins are labelled in blue. The proteins found in the dotted boxed area are listed on the right hand side of the figure. The expression levels of most detected OMPs do not change (apart from increased levels of OmpX and MipA in the strain expressing BamA$_{T434A}$). Statistical significance was determined using Persueus (see Methods).

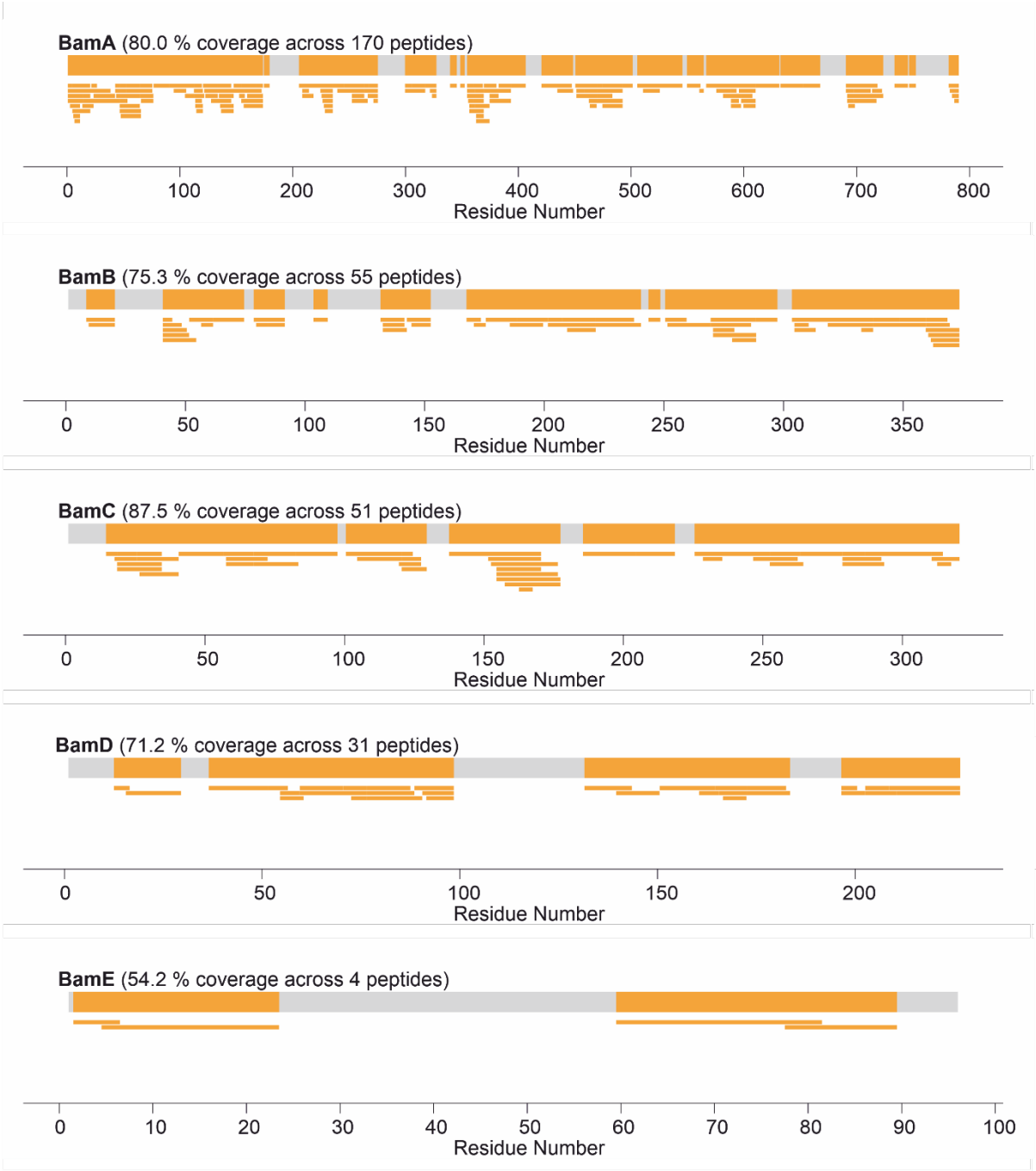

Supplementary Figure 9

Coverage maps of BAM subunits in HDX-MS experiments

The thick bar represents sequence coverage over each protein sequence, with regions shaded in orange or grey indicating regions that were covered or not covered by detected peptides, respectively. Small orange bars represent the individual peptides detected.

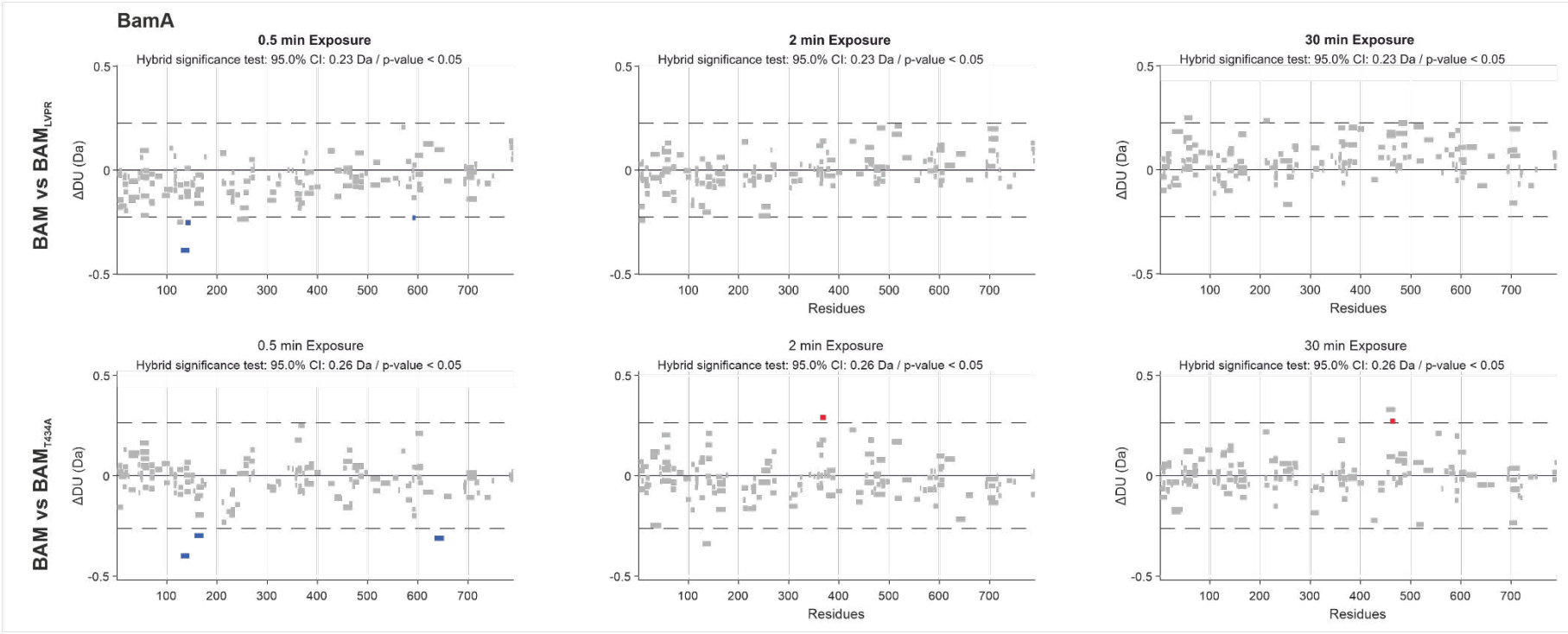

Supplementary Figure 10

HDX-MS data for BamA

Woods plots showing the differences in deuterium uptake in BamA subunits at three HDX timepoints (0.5, 2, 30 min), comparing BAM with either BAM_{LVPR} (top row) or BAM_{T434A} (bottom row). Woods plots were generated using Deuteros 2.0[10]. Peptides coloured in blue or red are protected or deprotected, respectively, from exchange in the BAM variant. Peptides with no significant difference between conditions, determined using a 95% confidence interval (dotted line), are shown in grey.

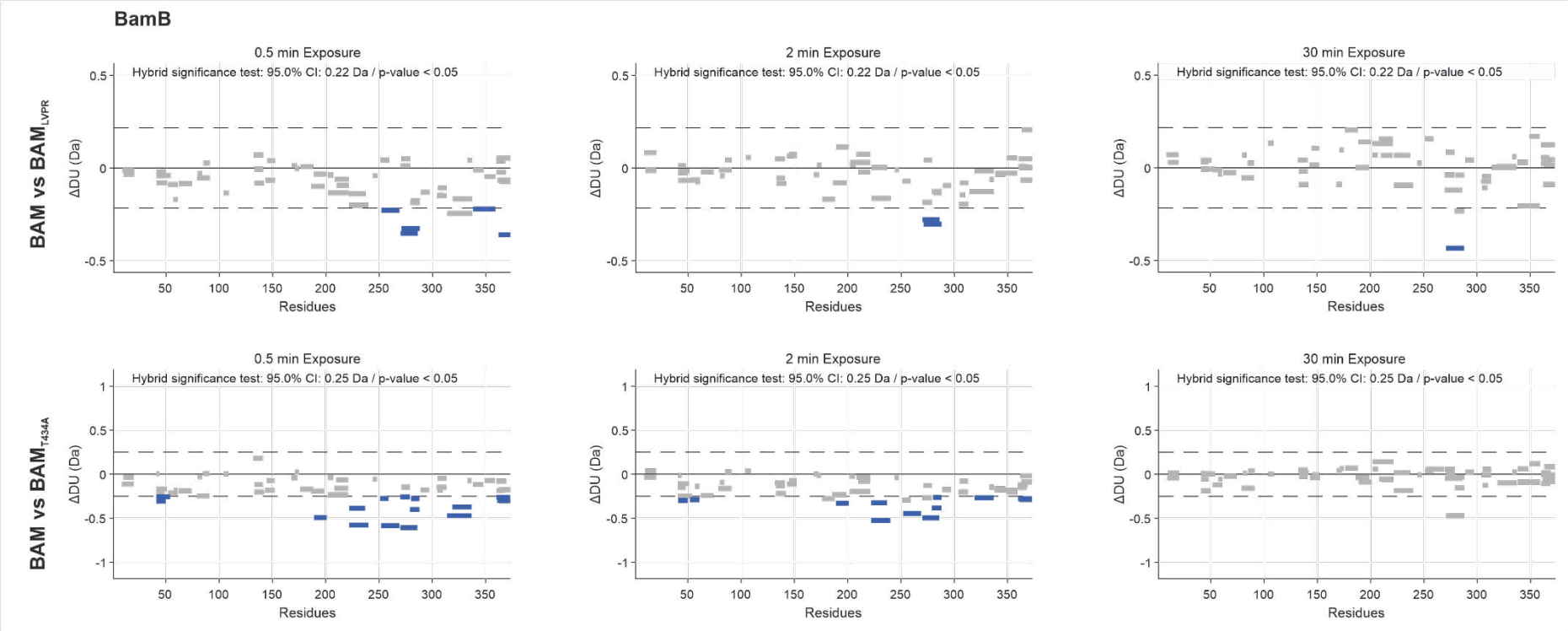

Supplementary Figure 11

HDX-MS data for BamB

Woods plots showing the differences in deuterium uptake in BamB subunits at three HDX timepoints (0.5, 2, 30 min), comparing BAM with either BAM_{LVPR} (top row) or BAM_{T434A} (bottom row). Woods plots were generated using Deuteros 2.0[10]. Peptides coloured in blue or red are protected or deprotected, respectively, from exchange in the BAM variant. Peptides with no significant difference between conditions, determined using a 95% confidence interval (dotted line), are shown in grey.

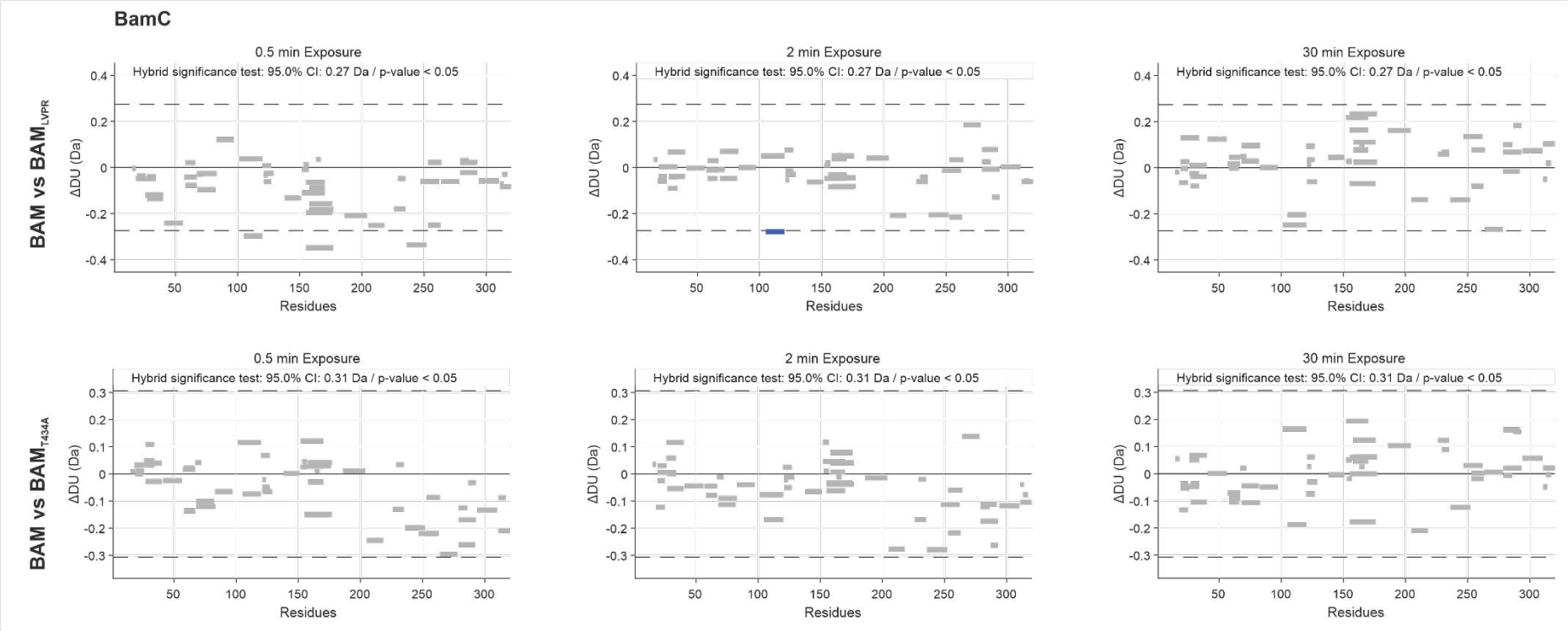

Supplementary Figure 12

HDX-MS data for BamC

Woods plots showing the differences in deuterium uptake in BamC subunits at three HDX timepoints (0.5, 2, 30 min), comparing BAM with either BAM_{LVPR} (top row) or BAM_{T434A} (bottom row). Woods plots were generated using Deuteros 2.0[10]. Peptides coloured in blue or red are protected or deprotected, respectively, from exchange in the BAM variant. Peptides with no significant difference between conditions, determined using a 95% confidence interval (dotted line), are shown in grey.

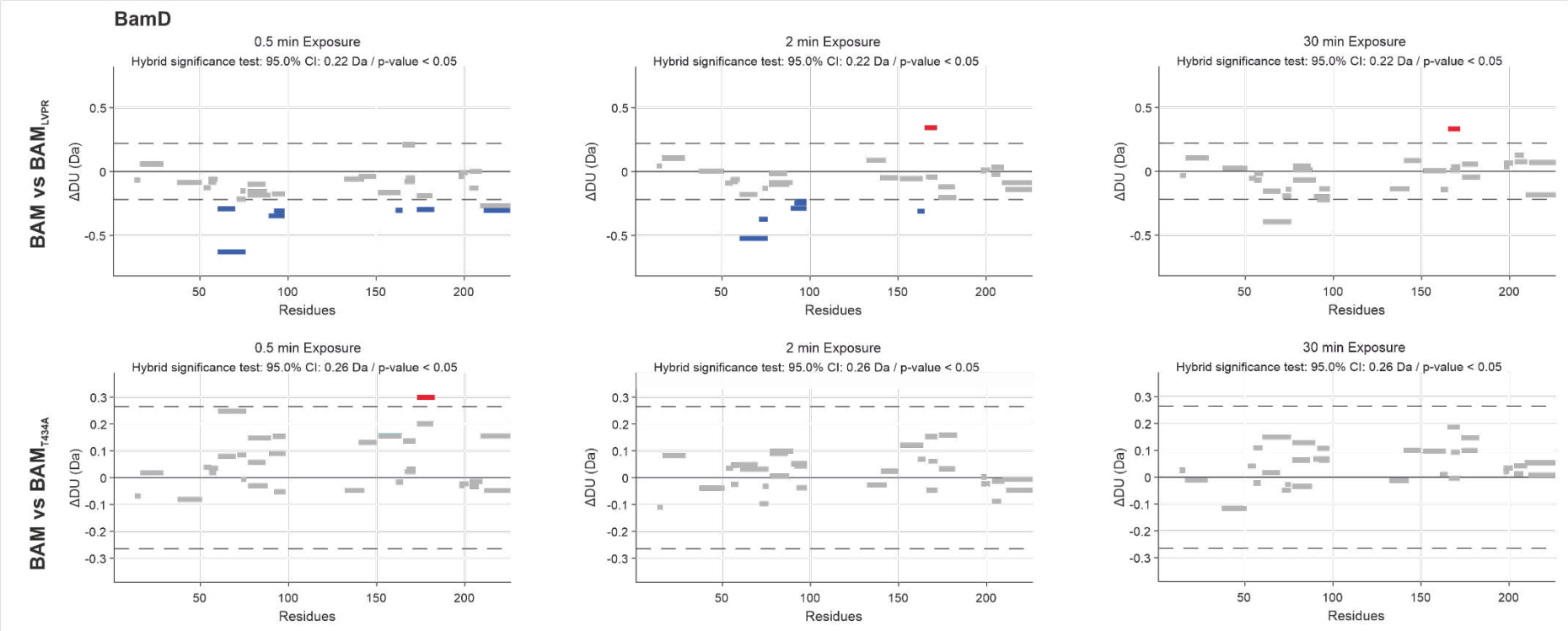

Supplementary Figure 13

HDX-MS data for BamD

Woods plots showing the differences in deuterium uptake in BamD subunits at three HDX timepoints (0.5, 2, 30 min), comparing BAM with either BAM_{LVPR} (top row) or BAM_{T434A} (bottom row). Woods plots were generated using Deuteros 2.0[10]. Peptides coloured in blue or red are protected or deprotected, respectively, from exchange in the BAM variant. Peptides with no significant difference between conditions, determined using a 95% confidence interval (dotted line), are shown in grey.

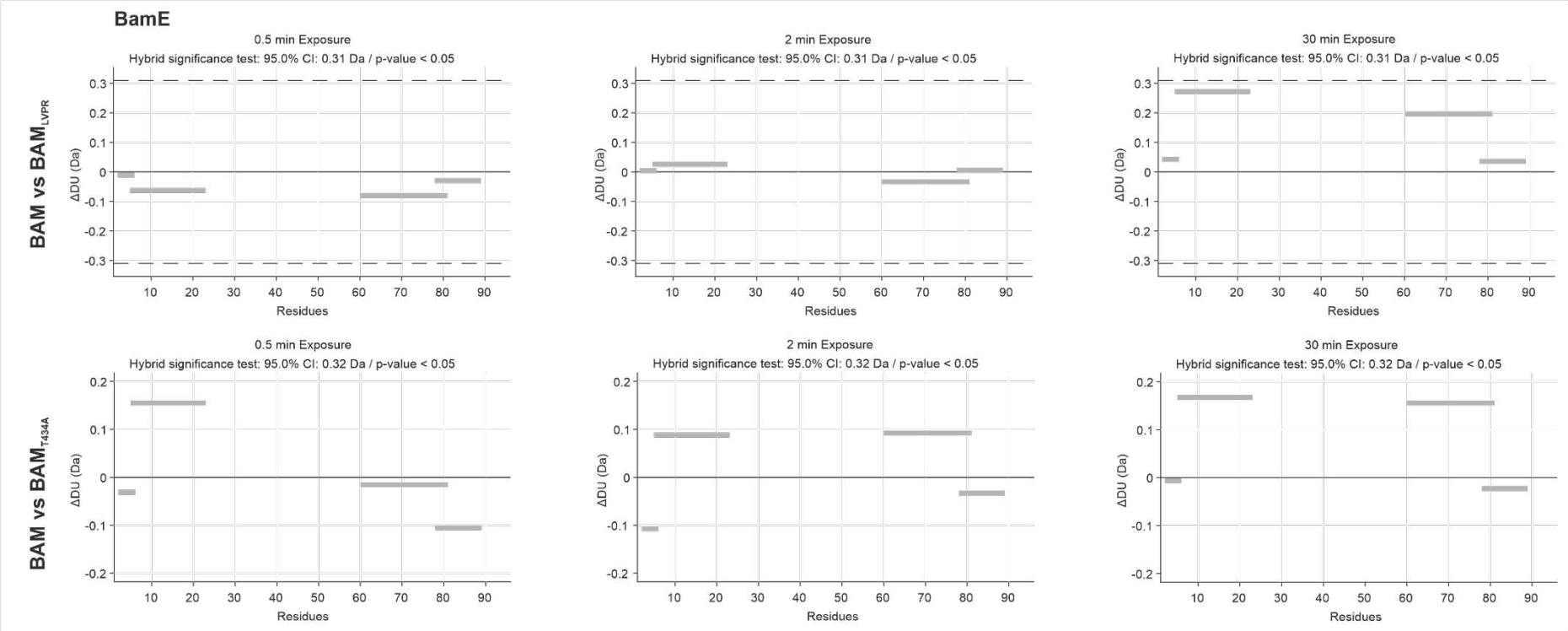

Supplementary Figure 14

HDX-MS data for BamE

Woods plots showing the differences in deuterium uptake in BamA subunits at three HDX timepoints (0.5, 2, 30 min), comparing BAM with either BAM_{LVPR} (top row) or BAM_{T434A} (bottom row). Woods plots were generated using Deuteros 2.0[10]. Peptides coloured in blue or red are protected or deprotected, respectively, from exchange in the BAM variant. Peptides with no significant difference between conditions, determined using a 95% confidence interval (dotted line), are shown in grey.

Supplementary References:

1 Majdalani, N., Hernandez, D. & Gottesman, S. Regulation and mode of action of the second small RNA activator of RpoS translation, RprA. *Mol Microbiol* **46**, 813-826, doi:10.1046/j.1365-2958.2002.03203.x (2002).

2 Ades, S. E., Grigorova, I. L. & Gross, C. A. Regulation of the alternative sigma factor sigma(E) during initiation, adaptation, and shutoff of the extracytoplasmic heat shock response in Escherichia coli. *J Bacteriol* **185**, 2512-2519, doi:10.1128/JB.185.8.2512-2519.2003 (2003).

3 Rodriguez-Alonso, R. *et al.* Structural insight into the formation of lipoprotein-beta-barrel complexes. *Nat Chem Biol* **16**, 1019-1025, doi:10.1038/s41589-020-0575-0 (2020).

4 Cho, S. H. *et al.* Detecting envelope stress by monitoring beta-barrel assembly. *Cell* **159**, 1652-1664, doi:10.1016/j.cell.2014.11.045 (2014).

5 Roman-Hernandez, G., Peterson, J. H. & Bernstein, H. D. Reconstitution of bacterial autotransporter assembly using purified components. *Elife* **3**, e04234, doi:10.7554/eLife.04234 (2014).

6 Csoma, N., Cho, S.-H., Collet, J.-F., & Bogdan I. BamAset: v0.2. *Zenodo*, doi: https://doi.org/10.5281/zenodo.13986908 (2025).

7 Haysom, S. F. *et al.* Darobactin B Stabilises a Lateral-Closed Conformation of the BAM Complex in E. coli Cells. *Angew Chem Int Ed Engl*, e202218783, doi:10.1002/anie.202218783 (2023).

8 Gu, Y. *et al.* Structural basis of outer membrane protein insertion by the BAM complex. *Nature* **531**, 64-69, doi:10.1038/nature17199 (2016).

9 Xiao, L. *et al.* Structures of the beta-barrel assembly machine recognizing outer membrane protein substrates. *FASEB J* **35**, e21207, doi:10.1096/fj.202001443RR (2021).

10 Lau, A. M., Claesen, J., Hansen, K. & Politis, A. Deuteros 2.0: peptide-level significance testing of data from hydrogen deuterium exchange mass spectrometry. *Bioinformatics* **37**, 270-272, doi:10.1093/bioinformatics/btaa677 (2021).